

SCALING OF SPATIAL AND TEMPORAL BIOLOGICAL VARIABILITY AT MARINE RENEWABLE ENERGY SITES

Dale A. Jacques
University of Washington
Seattle, Washington, USA

John K. Horne
University of Washington
Seattle, Washington, USA

¹Corresponding author: djacques@uw.edu

ABSTRACT

Baseline characterization of fish and macrozooplankton is required for marine renewable energy (MRE) site developments such as offshore wind, surface wave, and tidal power. Baseline measurements typically cover a small proportion of the total project area and need to be scaled to develop monitoring programs at pilot and commercial sites after installation. Spatial representativeness, the range to which observations from a point source can be interpolated, can be used to calculate the density of point source monitoring instruments. We demonstrate a framework for calculating the spatial representativeness of stationary splitbeam echosounders used to monitor pelagic fish and macrozooplankton at MRE sites by comparing observed variability between mobile and stationary acoustic surveys at a proposed MRE tidal site in Puget Sound, WA. Three approaches were used to test the consistency of spatial representativeness estimates. First, stationary observations of nekton variability were compared to mobile observations at different spatial scales to identify the scale at which similar patterns and variability were measured. Second, correlation coefficient models generated from spatial and temporal variograms and autocorrelation were used to describe the representativeness of point sources as a function of range. Spatial autocorrelation was used to show that nekton abundance measurements became independent at 300m, while temporal measurements became independent within 24 seconds. Third, an equation translating power law slopes of the spatial and temporal global wavelet spectrums, analogous to spectral densities, was used to translate variability between spatial and temporal measurement scales. Preliminary results indicate that spatial ($\text{Log}_{10}(\text{Wavelet Power}) = 1.24 + 0.223\text{log}_{10}(\text{meters})$) and temporal ($\text{Log}_{10}(\text{Wavelet Power}) = 0.74 + 0.405\text{log}_{10}(\text{hours})$) power laws are

equivalent at scales of approximately one month and 1 km. Subtracting these equations gives a scalar equation to translate between spatial and temporal variability across measurement scales. A standardized spatial representativeness calculation provides an objective technique to determine minimum monitoring effort, maximizes the cost effectiveness of monitoring for developers, and ensures adequate monitoring resolution for environmental regulators.

INTRODUCTION

Marine renewable energy (MRE) projects, such as wave and tidal power, continue to be developed despite the uncertainty of device and site effects on communities of fish and macrozooplankton (i.e. nekton)[1]. In part, this uncertainty has lead federal and state regulators to mandate biological monitoring at MRE sites, but sampling requirements for monitoring programs are inconsistent among sites [2]. Determining monitoring requirements for individual projects has resulted in delays and increased costs of development and permitting [3]. Regulatory specifications and procedures using quantitative protocols are needed to determine sampling effort for monitoring programs and will result in streamlined permitting and development for both regulators and developers.

The objective of biological monitoring is to identify effects of development on aquatic organism species within the community. An effect is defined as one or more statistically significant changes between baseline and post-perturbation measurements of the mean or variance of biologically relevant metrics [4, 5]. The objective of MRE site monitoring, which focuses on changes such as nekton density over the entire domain, is to identify effects changing the health and stability of components or the entire ecosystem. Domain level MRE biological monitoring programs collect baseline measurements of nekton density,

variability, and distribution before deployment of devices and then compare them to post-installation measurements as a site progresses from a pilot to a commercial array. Long term, post-perturbation measurements can be collected from vessel-based, mobile surveys, or from autonomous, stationary instrument packages. Stationary instrument packages are assumed to be more cost effective over the lifetime duration of MRE monitoring programs due to labor, fuel, and ship time costs associated with mobile surveys. Stationary surveys that produce temporally-indexed data at single location have the added ability to monitor temporal variability at finer resolutions and higher precision than possible using data from repeated, mobile surveys.

Temporally-indexed data are not without constraints. Stationary surveys characterize temporal variability, but the spatial variability of ecosystem components is not quantified and cannot be ignored [6]. Non-uniform (i.e. patchy [7]) nekton distributions limit the spatial accuracy of a temporally-indexed data series, as spatial variability in fish habitat and density increases with spatial scale (i.e. red, pink, or Brownian noise)[8, 9, 10]. As the aerial footprint of an MRE site increases from pilot to commercial scale, spatial heterogeneity of fish habitats and densities are expected to increase, with the potential for concomitant increases in deleterious effects. At spatial scales exceeding those of homogeneous organism distributions [11], a single, stationary monitoring package is no longer adequate to characterize fish densities and dynamics of the MRE site. Additional monitoring packages will be required to quantify spatial variability, which also increases the statistical power to detect change [5, 12] within a spatial domain. One major challenge in the design of monitoring programs is to determine the density of instrument packages required to detect change in variables specified in operating licenses.

An ideal statistical method used to calculate the density of sampling packages needed to monitor a MRE site would optimize the amount of data collected and, at the same time, optimize the cost of collecting measurements. For monitoring programs using moored or bottom-deployed instrument packages, there is a need to determine the corresponding spatial area that a point source measurement represents, referred to in the literature as the 'spatial representativeness' [11, 13]. The area a point represents is dependent on the spatial variability surrounding the location, and the scale at which it is measured [9, 10]. The variance of a measurement series is expected to increase with both spatial and temporal scale in most biological circumstances [9]. The power

spectrum can be used to quantify the variance of a data series as a function of frequency or scale [14]. Assuming that variability increases with scale, measurements are expected to become less correlated with range from a location [15]. Correlations have been documented between spatial and temporal scales over which physical and biological processes operate (Appendix A) [9, 16, 17]. If these linkages exist, then there will be a relationship between the spatial and temporal spectra of the variable or metric used to monitor change [17]. Using these principles, the autocovariance of measurements in space and time can be used to estimate the spatial representativeness of temporally-indexed, point source measurements.

Here, acoustic data used to index nekton densities during a baseline study density at a proposed MRE site in Admiralty Inlet, Puget Sound, WA are used as a case study to compare estimates of spatial representativeness using three methods. Spatially- and temporally-indexed nekton density and variance measurements at two discrete spatial scales are used to determine relationships between spatially and temporally-indexed data. Since both the mean [5] and variance [4] of variables are appropriate monitoring metrics, the spatial representativeness of the mean and variance of nekton density are estimated separately. This analysis initiates efforts to scale point source monitoring measurements to the domain of a MRE commercial site and to optimize metric selection and monitoring costs.

METHODS

Data Collection

Spatially- and temporally-indexed acoustic surveys were used to measure baseline nekton densities at a proposed tidal MRE pilot site in Admiralty Inlet, Puget Sound, WA. Admiralty Inlet is a shallow sill at the entrance to Puget Sound in which tidal currents exceed 3.5 m/s. The proposed pilot site is located ~750m off Admiralty Head in ~55m of water. Active acoustics were chosen to measure nekton density because they are robust to many of the sampling challenges introduced by strong tidal currents, such as turbulence and turbidity, which limit or inhibit other types of traditional biological measurements. The high spatial and temporal resolution of acoustic measurements is ideal for quantifying spatial representativeness. Both acoustic surveys were conducted using 120 kHz splitbeam echosounders with a -75dB threshold. Measurements were constrained to within 25m of the bottom, representing approximately twice the hub-height of the proposed tidal turbine, to

facilitate a relevant, direct comparison between the two series. Fish and macrozooplankton density were measured using mean volume backscattering strength (S_v) [18], a log-normalized acoustic estimate of nekton density.

Mobile Survey

Two spatially-indexed acoustic surveys were conducted from May 2nd to May 13th and June 3rd to June 14th, 2011. Each survey repeatedly sampled two grids of transects, one north and one south of the proposed pilot site, at both day and night. A total of 57 sampling grids were completed over both surveys encompassing both grids, day and night, and all tidal states, covering 547 transects. Transects were oriented perpendicular to the shore and the flow of the predominant tidal current (Figure 1), and were surveyed at approximately seven knots. The grids cumulatively covered 16.1 km² with transects spaced ¼ km apart near the proposed pilot site radiating to lower resolution transects spaced ½ km apart. The echosounder used during the spatially-indexed survey sampled depths from ~20m to ~100 m, but analysis was constrained to within 25m of the bottom.

Spatially indexed acoustic data were sampled at 1 Hz using a 120 kHz transducer with a 7° beam width (between half power points), transmitting at 500 Watts for a 512 ms pulse duration. Surface turbulence due to tidal currents was a major

feature in the acoustic data record and was identified using the schools detection algorithm in Echoview (v5.4.91 Myriax Inc.) acoustic data processing software. School detection parameter settings were: minimum total school length = 5m, minimum total school height = 3m, minimum candidate length = 5m, minimum candidate height = 3m, maximum vertical linking distance = 10m, and maximum horizontal linking distance = 10m. Identified schools that intersected the 3m depth exclusion range were excluded as surface turbulence. Noise was removed from the data using a -75 dB threshold, which corresponded to a 16 dB signal to noise ratio. The threshold was set to assist the turbulence removal algorithm and to exclude microzooplankton from the analysis. The echosounder was calibrated using a tungsten carbide sphere following the protocols outlined in Foote et al.[19].

Spatial data were analyzed at 20m and 300m horizontal resolutions depending on the analysis. Analyses not requiring independence between samples were analyzed at 20m horizontal resolution, encompassing ~6 pings per bin. Autocorrelation functions determined spatial data became independent and identically distributed at 300m. At least five independently distributed 300m data bins were nested within each transect.

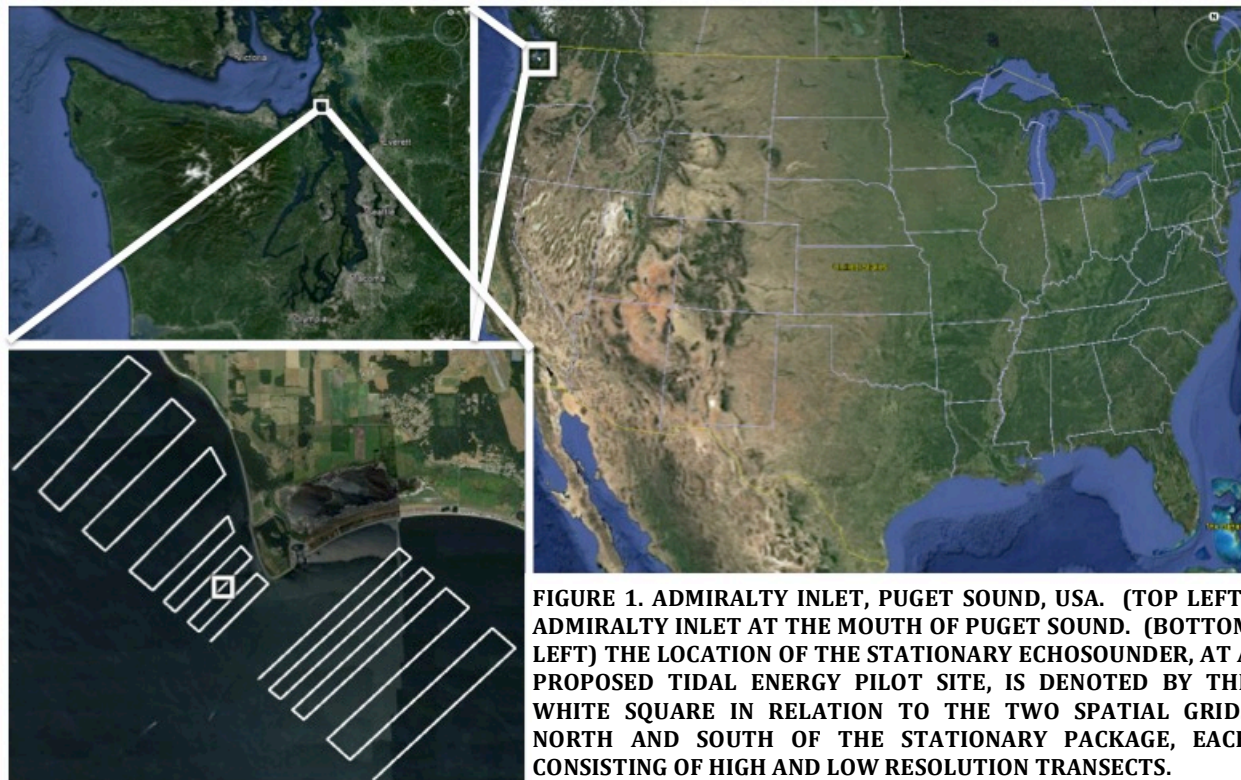


FIGURE 1. ADMIRALTY INLET, PUGET SOUND, USA. (TOP LEFT) ADMIRALTY INLET AT THE MOUTH OF PUGET SOUND. (BOTTOM LEFT) THE LOCATION OF THE STATIONARY ECHOSOUNDER, AT A PROPOSED TIDAL ENERGY PILOT SITE, IS DENOTED BY THE WHITE SQUARE IN RELATION TO THE TWO SPATIAL GRIDS NORTH AND SOUTH OF THE STATIONARY PACKAGE, EACH CONSISTING OF HIGH AND LOW RESOLUTION TRANSECTS.

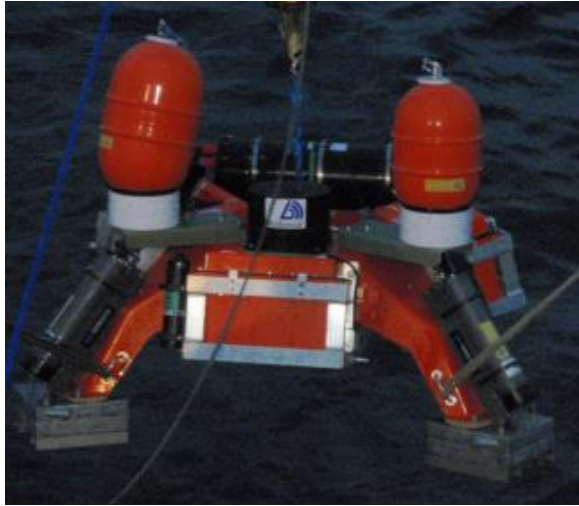


FIGURE 2. PICTURE OF THE STATIONARY, BOTTOM DEPLOYED 120 KHZ SPLITBEAM ECHOSOUNDER.

Stationary Survey

An autonomous, bottom deployed, upward facing 120 kHz splitbeam echosounder sampled at 5 Hz for 12 minutes on a 2 hour duty cycle from May 10th to June 9th, 2011 (Figure 2). Similar to the spatial survey, the transducer had a 7° beam angle (between half power points) and transmitted at 1000 Watts. The stationary echosounder was deployed at the location of the proposed pilot energy site, located in the high-resolution portion of the north spatial survey grid in ~55m of water and ~750m from Admiralty Head. Noise was removed using a -75 dB threshold, identical to the spatial survey, and data was constrained to 25m from the bottom.

A total of 360 12-minute sampling periods were collected over the 30-day deployment. Stationary data was analyzed at either 1.2-second or 24-second temporal resolution depending on the analyses. A total of 600, 1.2-second bins and 30 24-second bins were nested within each 12-minute cycle. Six pings were included in each 1.2-second temporal bin; approximately equal to the number of pings in the fine resolution (20m) spatial data. Stationary data were determined to be independent at 24 seconds using autocorrelation functions. A 24-second stationary bin (120 pings) had a similar number of pings as a 300m spatial bin (~85 pings depending on vessel speed).

Analysis

Three methods were used to estimate spatial representativeness of nekton density measurements: 1) a direct comparison of concurrent mobile and stationary measurements at two spatial scales; 2) a correlation coefficient model; and 3) a translation between spatial and temporal spectra.

Direct Comparison of Concurrent Measurements

The mean and variance of nekton density from concurrent temporally- and spatially-indexed measurements in close proximity were compared at two scales:- transect and grid. Concurrent measurements were limited to spatial measurements collected within the high-resolution portion of either the north or south grid. Of all transects surveyed, only eight transects and five spatial grids met these requirements. The discrepancy in sampling size is due to three grids containing multiple concurrent transects.

Temporally-indexed nekton densities were averaged within each 12-minute sampling cycle. The thirty, 24 second bins within each cycle were used to calculate the mean and standard deviation of density measurements. The mean and standard deviation of fish and macrozooplankton densities from the spatial survey were calculated from all 300m bins in either the transect or grid of the concurrent observation. Each transect was composed of at least four complete 300m spatial bins. Each grid was composed of approximately ninety-four 300m spatial bins.

Concurrent measurements in space and time were regressed using a least squares linear model. The scale at which the model most closely resembled the theoretical 1:1 relationship ($Y = X + 0$) between spatial and mobile measurements was selected as being the most similar. This method cannot determine the precise spatial representativeness of the stationary device, but suggests which spatial scale the stationary measurements most closely represent.

Scaling means: Correlation Coefficient Model

A correlation coefficient model was used to describe how representative measurements were as a function of range from a location following Anttila et al. [11]. Correlation coefficients were calculated as a function of range, and squared to yield a coefficient of determination (R^2), the proportion of variability explained by correlation. Correlation coefficient models were constructed for each transect, from data exported at a 20m resolution. The coefficient of determination for all transects ($n = 547$) were averaged at each range. A power law was fit to these averages, (i.e. the theoretical autocorrelation structure in red noise [15]), using a least squares model. Two thresholds were used to determine representativeness. A predetermined threshold of $R^2 = 0.50$ was taken from [11], which developed this technique for water quality monitoring in inland lakes. A second threshold was statistically derived from the 95% significance level of lagged

correlation coefficients. Assuming a random data series, lagged-correlation coefficients are distributed around zero with a variance of $1/n$, with n the length of the data series. The 95% confidence interval of lagged correlation coefficients is $2/\sqrt{n}$. Since correlation coefficients were calculated for each transect, the median data series length of all transects was used (2600 meter transect sampled at a 20m resolution, yielding $n = 130$ samples). Therefore the 95% CI for a lagged correlation coefficient given the median transect length was 0.175. Squaring the lagged correlation coefficient 95% CI yields the 95% CI for the coefficient of determination, which was 0.03 for our data. This threshold corresponds to the range at which observations became approximately statistically independent.

Scaling Variability: Translating between Spatial and Temporal Spectra

The spatial scale at which temporal variability can be considered representative can be calculated from the relationship between spatial and temporal variability. Given that processes operating over larger spatial scales usually occur at larger temporal scales (Appendix A; excluding highly predictable celestial events such as tides and diel periods) [9, 16, 20], it is reasonable for longer temporal measurements to represent larger spatial scales. Equivalent spatial and temporal scales will observe equivalent amounts of variability. Using the relationship between spatial and temporal spectra, the variance at the largest temporal scale analyzed up to $\frac{1}{2}$ of the time-series (Nyquist frequency [14]), and then translated to a spatial scale. At these coincident scales, we expect to see identical amounts of spatial and temporal variability. As the largest temporal scale of our monitoring increases, the spatial scale to which it is representative will also increase.

Wavelet analysis simultaneously decomposes a data series into time and frequency domain to analyze localized deviations from the expected spectral power [21]. By averaging across times, the global wavelet spectrum is mathematically equivalent to the power spectra [22, 23, 24]. A global wavelet spectra was calculated for all 547 spatial transects and 360, 12-minute temporally-indexed periods using the high-resolution data. The mean global wavelet power was then calculated at each spatial and temporal scale. Global wavelets were calculated using a Morlet wavelet ranging from the minimum resolution to the Nyquist frequency (see [21] for discussion). Global wavelet power was calculated as a function of scale instead of frequency to standardize irregularities in transect length. Both wavelet

power and scale were log normalized, and a best fit line was regressed using linear least squares for both spatially- and temporally-indexed data. These best-fit lines were then used to calculate the spatial scale at which an equivalent amount of variance was measured at the largest temporal scale.

Lagged coefficient of determinations, used in the spatial correlation coefficient model above, are equivalent to the square of the autocorrelation function. The autocorrelation function is the autocovariance standardized to the variance of the series. The power spectrum is the Fourier cosine transform of the autocovariance [14]. The spatial correlation coefficient model and the comparison of spectra are mathematically linked, but this method allows for the direct comparison between spatial and temporal variability.

RESULTS

Direct Comparison of Concurrent Measurements

Temporally-indexed measurements of nekton were significantly correlated to spatially-indexed

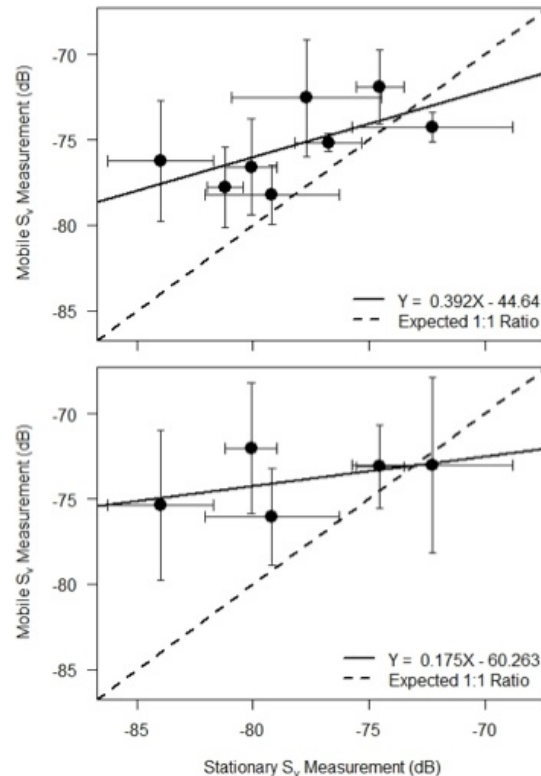


FIGURE 3. DIRECT COMPARISON OF CONCURRENT SPATIAL AND TEMPORAL MEASUREMENTS OF FISH AND MACROZOOPLANKTON DENSITY AT THE (TOP) TRANSECT AND (BOTTOM) GRID SPATIAL SCALE. THE DASHED LINES ARE THE THEORETICAL 1:1 RELATIONSHIP BETWEEN SPATIAL AND TEMPORAL MEASUREMENTS, THE STANDARD USED TO COMPARE THE BEST-FIT LINES. ERROR BARS ARE ONE STANDARD DEVIATION.

measurements at both transect and grid spatial scales (Figure 3). Although the slopes of both lines were significantly greater than zero, they were well below the theoretical slope of a 1:1 relationship. Using a 1:1 relationship ($Y = X + 0$) between spatial and temporal measurements as a standard, nekton density within a single transect was more strongly related to stationary measurements than nekton densities within a grid. The slope of the transect scale comparison line ($m = 0.392$) was more than twice the slope of the same comparison done at the grid scale ($m = 0.175$). The intercept of the transect scale comparison was ~25% smaller than at the grid scale ($b = -44.64$ and -60.263 , respectively). Qualitatively the variance of each measurement, denoted by error bars, looks to be roughly correlated between mobile and spatial surveys, but more highly correlated at the transect level.

Spatial Correlation Coefficient Model

The representativeness of nekton density measurements decayed rapidly in space (Figure 4). Less than half the variability in nekton density could be explained beyond 20m. As in traditional autocorrelation, representativeness at range 0 is 1. Ideally, a statistical model of representativeness would start at range 0, but representativeness decayed so rapidly within the first 20m that that a power law fit using the perfectly correlated data at range 0 overestimated the representativeness of measurements within 40m, and underestimated the representativeness beyond 40m (Figure 4, top). To model the decay, the power law was not constrained through a representativeness of 1 at range 0. After 20m, the representativeness decayed following a power law ($Y = 0.3392e^{-0.168X}$), where X is the number of 20m lags and Y is the representativeness (Figure 4, bottom).

The range at which observations are representative can be calculated using the predetermined thresholds of representativeness, $R^2 = 0.5$ and 0.03 , and solving for the range (X) in the spatial correlation coefficient model. Unfortunately, $R^2 = 0.50$ falls within the first 20m, where the power law model breaks down. Linear interpolation between range 0 and range 20m suggests a representative range of 15m at the $R^2 = 0.5$ threshold. The spatial representativeness calculated at the $R^2 = 0.03$ threshold is 300m. Variability of representativeness estimates between transects decreased with range. Over tidal cycles, autocorrelation did not change significantly in slack or extreme tide states ($<0.5\text{m/s}$ and $>1.5\text{m/s}$, respectively) in either the mobile or stationary surveys (Figure 5).

Comparison of Spatial and Temporal Spectra

As expected, spatial and temporal spectra of nekton density increased with scale (Figure 6). The intercept of the resulting spatial and temporal best-fit spectral lines are almost identical, suggesting that variability within a 1.2 second bin and 20m spatial bin are equivalent. The spectral power in both the stationary and mobile data sets increased with scale, consistent with a traditional red or pink spectra. Variability surrounding the spectra remained consistent across both spatial and temporal series and across scales.

The log normalized global wavelet power at the Nyquist frequency of the temporal spectra was 1.524. An equivalent amount of variability occurred at 688m spatial scales in the spatial spectra. The spatial representativeness of a 12 min temporal measurement is 688m when scaled using nekton variability. This range is more than double that determined by the correlation in means, but is consistent with the conclusion from the direct comparison analysis that the equivalent

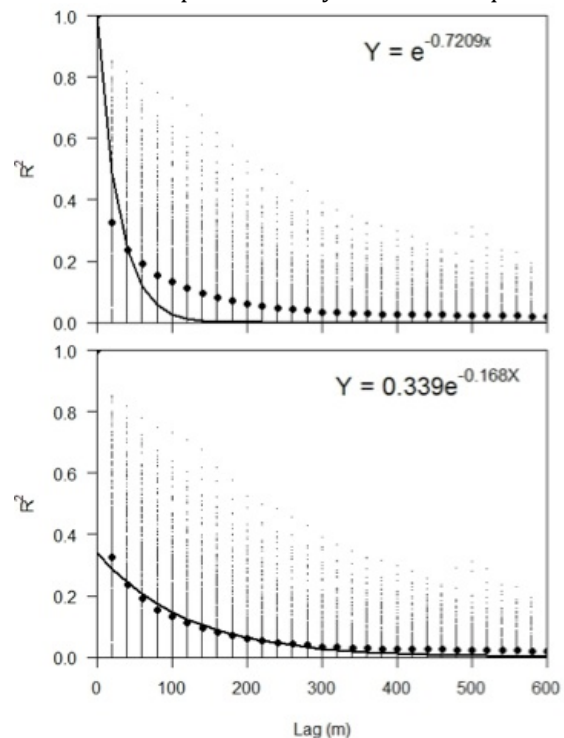
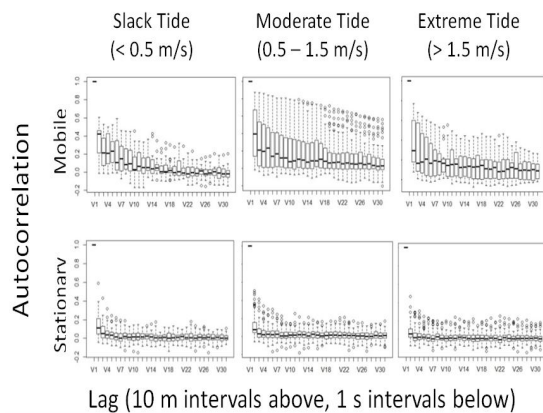


FIGURE 4. COEFFICIENT DETERMINATION OF FISH AND MACROZOOPLANKTON DENSITY AS A FUNCTION OF DISTANCE. EACH SMALL DOT REPRESENTS THE MEAN COEFFICIENT OF DETERMINATION AT A SPECIFIC RANGE WITHIN A SINGLE SPATIAL TRANSECT. FILLED CIRCLES ARE THE MEAN COEFFICIENT OF DETERMINATION FOR THAT RANGE, AND THE BEST-FIT LINE IS MODELED USING A POWER LAW THAT IS (TOP) CONSTRAINED THROUGH 1 AT A RANGE-0 (PERFECTLY CORRELATED WITH ITSELF) OR (BOTTOM) UNCONSTRAINED.



Lag (10 m intervals above, 1 s intervals below)

FIGURE 5. AUTOCORRELATION IN NEKTON DENSITIES OBSERVED ACROSS EXTREME, MODERATE, AND SLACK TIDAL CURRENTS IN BOTH THE SPATIALLY- AND TEMPORALLY-INDEXED SURVEY. BOXES ENCOMPASS DATA WITHIN THE INTERQUARTILE RANGE AND EXTEND TO 1.5 TIMES THE INTERQUARTILE RANGE.

spatial scale must be smaller than that of a transect.

DISCUSSION

Point measurements of mean nekton density were estimated as being representative of 15 or 300m, depending on the coefficient of determination threshold chosen for “representativeness”. These ranges translate to site-monitoring instrument densities of 1,414.78 or 3.56 instruments per square kilometer. Obviously, it would not be economically viable to develop regulations requiring 1,414.78 instruments per square kilometer, but the method (spatial correlation coefficient models) and threshold ($R^2 = 0.5$) used to calculate this number were derived from monitoring water quality in a lake, which varies over much larger spatial scales relative to distributions of aquatic organisms [7, 11]. We have proposed a new statistical technique to calculate a coefficient of determination threshold more suitable for biological monitoring. Using this technique, a coefficient of determination threshold of 0.03 was used, which correlates to the distance at which horizontal nekton density measurements became statistically independent. This threshold, dependent in part on the baseline monitoring effort, appears to be more economically viable for biological monitoring and a more realistic expectation for regulators.

The spatial representativeness of the variance, 688m, was more than double the range of the mean representativeness and equates to only 0.68 instruments per square kilometer. An important caveat to scaling temporal to spatial variance is that the linearity of both the spatial

and temporal spectra must be validated before scaling variability. The linear relationship of the spatial or temporal spectra cannot be extrapolated beyond the scales that have been directly measured. Deviations from linearity, will compromise estimates of spatial representativeness. Estimating spatial representativeness requires a dedicated baseline survey that exceeds the spatial and temporal scales used to translate variability.

The number of stationary monitoring instruments will increase as the aerial footprint of the MRE site increases to insure adequate spatial monitoring, with concomitant increases in monitoring program cost. The MRE industry is striving to remain cost competitive with traditional energy sources, having the benefit of established infrastructure, standardized monitoring regulations, and economical source material (e.g. natural gas). MRE monitoring programs must remain cost effective as a site scales from a pilot to a commercial scale. One way to minimize monitoring costs is to minimize the number of monitoring packages. An obvious statement with potentially large impact. Current costs to engineer, deploy, maintain, retrieve, and analyze a stationary echosounder package has been estimated at \$250,000 [25]. Without objective methods to estimate sampling effort, regulators are forced to use best guesses about the efficacy of proposed monitoring. Uninformed regulatory specifications lead to two possible outcomes: either an excess of monitoring instruments, which unnecessarily increases monitoring costs, or too few monitoring instruments, which would lower the probability of detecting biological effects. Biological monitoring is a significant cost of MRE projects [3], but it should not be the factor that inhibits the growth of a new industry sector that is competing with established energy providers.

It should be noted that many current MRE monitoring programs are focused on directly observing or quantifying specific interactions between individual organisms and MRE devices. Although these programs are more effective at quantifying the effect of devices on individual organisms due to a specific stressor (e.g. direct strike or impingement), they cannot detect if the biological community as a whole has been affected. Although there is a need for near-device monitoring, this paper presents multiple methods to determine the optimal instrument density for domain monitoring using point source instruments.

The longevity of scaling equivalents is uncertain and an interesting question in itself. Previous studies [6,11,13], limited in number,

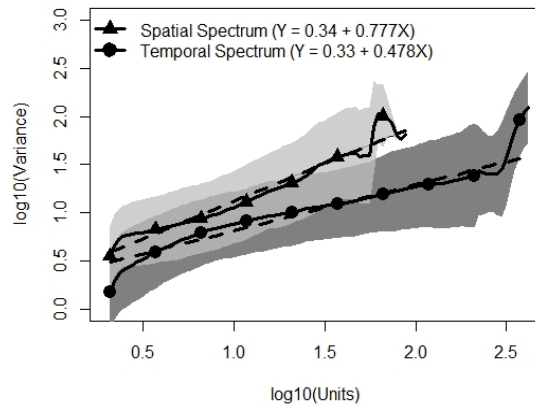


FIGURE 6. SPATIAL AND TEMPORAL SPECTRA OF FISH AND MACROZOOPLANKTON DENSITY. SPATIAL UNITS WERE 20M, TEMPORAL UNITS WERE 1.2 SEC. SOLID LINES ARE THE AVERAGE SPECTRUM AT A GIVEN SCALE, DASHED LINES ARE THE CORRESPONDING BEST FIT LINES. SHADED POLYGONS ENVELOPE THE MEAN SPECTRA +/- ONE STANDARD DEVIATION.

focus on the spatial representativeness of temporally indexed measurements, but none have investigated the temporal representativeness of spatially indexed measurements. In theory, these scaling factors could be inverted to calculate the temporal representativeness of spatial measurements.

To determine the spatial equivalence of point location, temporally-indexed data for use in long term biological monitoring programs, we recommend pre-installation baseline studies measuring both spatial and temporal variability in any and all potential monitoring metrics. This baseline study is an essential component of site characterization requirements.

CONCLUSIONS

1). Both spatially- and temporally-indexed baseline surveys are needed to establish monitoring programs. In this case, both spatial and temporal variability of nekton density were measured to estimate the area that data from a stationary, bottom-mounted echosounder represents. The only way to measure both spatial and temporal variability is to conduct two separate surveys simultaneously. Although initially costly, estimating spatial representativeness of point source data will objectively determine the required density of monitoring instruments and reduce long-term costs of the monitoring program.

2). The methods presented in this paper are flexible and objective dependent. Biological or physical variables can be used as monitoring

metrics to detect change in a quantity of interest. This approach can be applied to monitoring programs that focus on either the mean or variance of a quantity, giving developers and regulators the flexibility to identify which metric(s) are best suited to detect significant change at each MRE site.

3). This paper presents a quantitative method to estimate the density of stationary packages needed to monitor an MRE site. This method simplifies the design of a monitoring program and can be used to objectively determine the monitoring expectations of regulators and responsibility of developers. Given appropriate spatial and temporal data, regulators can use this approach to calculate and specify the number of monitoring packages as part of site permitting and licensing .

ACKNOWLEDGEMENTS

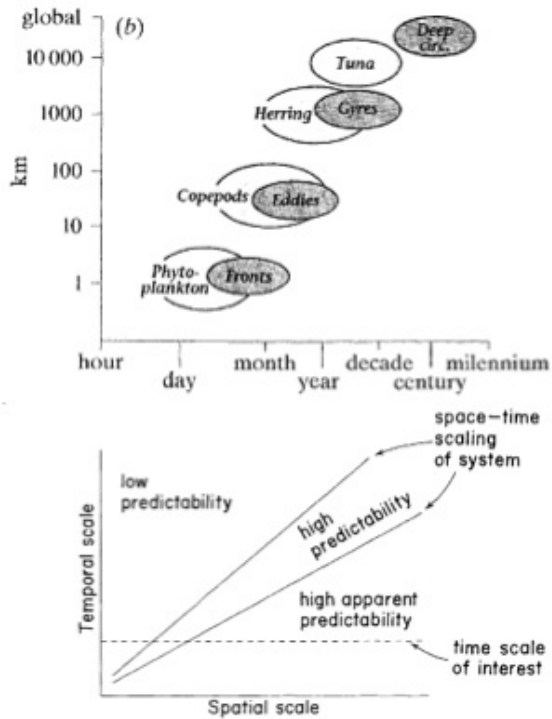
Thanks to the captain and crew of the R.V. Centennial for ship operations in Admiralty Inlet. Thanks to Jen Nomura, David Barbee, and Sandra Parker-Stetter for assistance in the field and to Hannah Linder for assisting with data processing. Funding was provided by U.S. Department of Energy, U.S. Bureau of Ocean Energy Management, under the National Oceanic Partnership Program, and the National Science Foundation.

REFERENCES

- [1] Polagye, B., Van Cleve, B., Copping, A., Kirkenhall, K. 2011. "Environmental Effects of Tidal Energy Development," U.S. Department of Commerce, NOAA Technical Memo, NMFS F/SPO, pp.186.
- [2] FERC. 2006. "Policy Statement on Hydropower Licensing Settlements," Settlements in Hydropower Licensing Proceedings Under Part I of the Federal Power Act, Docket No. PL06-5-000 pp. 19.
- [3] Copping, A.E., Geerlofs, S.H. 2011. "The Contribution of Environmental Siting and Permitting Requirements to the Cost of Energy for Marine and Hydrokinetic Devices," PNNL-20963, pp. 21.
- [4] Underwood, A. J. 1991. "Beyond BACI: Experimental Designs for Detecting Human Environmental Impacts on Temporal Variations in Natural Populations," Marine and Freshwater Research, **42**(5), pp. 569-587.
- [5] Osenberg, C. W., Schmitt, R.J., Holbrook, S.J., Abu-Saba, K.E., and Flegal, R.A. 1994. "Detection of Environmental Impacts: Natural Variability, Effect Size, and Power Analysis," Ecological Applications, **4**(1), pp. 16-30.

- [6] Ciach, G. J., and Krajewski, W. F. 2006. "Analysis and Modeling of Spatial Correlation Structure in Small-scale Rainfall in Central Oklahoma," *Advances in Water Resources*, **29**(10), pp. 1450–1463.
- [7] Horppila, J., Peltonen, H., Malinen, T., Luokkanen, E., Kairesalo, T. 1998. "Top-down or Bottom-up Effects by Fish: Issues of Concern in Biomanipulation of Lakes," *Restoration Ecology*, **6**(1), pp. 20-28.
- [8] Platt, T., and Denman, K.L., 1975. "Spectral Analysis in Ecology," *Annual Review of Ecology and Systematics*, pp.189–210.
- [9] Wiens, J. A. 1989. "Spatial Scaling in Ecology." *Functional Ecology*. **3**(4), pp. 385–397.
- [10] Levin, S. 1992. "Promoting the Science of Ecology," *Ecology*, **73**(6), pp. 1943–1967.
- [11] Anttila, S., Kairesalo, T., and Pellikka, P. 2008. "A Feasible Method to Assess Inaccuracy Caused by Patchiness in Water Quality Monitoring," *Environmental Monitoring and Assessment*, **142** (1), pp. 11–22.
- [12] Mapstone, B. D. 1995. "Scalable Decision Rules for Environmental Impact Studies: Effect Size, Type I, and Type II Errors," *Ecological Applications*, **5**(2), pp. 401–410.
- [13] Janis, M., and Robeson, R. 2004. "Determining the Spatial Representativeness of Air-Temperature Records Using Variogram-Nugget Time Series," *Physical Geography*, **25**(6), pp. 513–530.
- [14] Denman, K.L. 1975. "Spectral Analysis: A Summary of the Theory and Techniques," *Canadian Fisheries and Marine Service Technical Report No. 539*, pp. 37.
- [15] Gilman, D.L., Fuglister, F.J., Mitchell Jr., J.M. 1962. "On the Power Spectrum of "Red Noise"," *Journal of the Atmospheric Sciences*, **20**, pp. 182-184.
- [16] Steele, J. H., Henderson, E.W., Mangel, M., and Clark, C. 1994. "Coupling Between Physical and Biological Scales [and Discussion]," *Philosophical Transactions of the Royal Society of London. Series B: Biological Sciences*, **343**(1303), pp. 5–9.
- [17] De Santis, A., Barraclough, D.R., and Tozzi, R. 2003. "Spatial and Temporal Spectra of the Geomagnetic Field and Their Scaling Properties," *Physics of the Earth and Planetary Interiors*, **135**(2–3), pp. 125–134.
- [18] MacLennan, D. N., Fernandes, P. G., and Dalen, J. 2002. "A Consistent Approach to Definitions and Symbols in Fisheries Acoustics," *ICES Journal of Marine Science: Journal Du Conseil*, **59**(2), pp. 365–369.
- [19] Foote, K., Knudsen, H., Vestnes, G., MacLennan, D., and Simmonds, E. 1987. ". Calibration of acoustic instruments for fish density estimation: a practical guide," *ICES Cooperative Research Report*, **144**, pp. 57.
- [20] Stommel, H. 1963. "Varieties of Oceanographic Experience: The Ocean Can Be Investigated as a Hydrodynamical Phenomenon as Well as Explored Geographically." *Science*, **139**(3555), pp. 572–576.
- [21] Torrence, C., and Compo, G.P. 1998. "A Practical Guide to Wavelet Analysis," *Bulletin of the American Meteorological Society*, **79**(1) (January), pp. 61–78.
- [22] Hudgins, L., Friehe, C.A., Mayer, M.E. 1993. "Wavelet Transforms and Atmospheric Turbulence," *Physical Review Letters*, **71**, pp. 3279-3282.
- [23] Percival, D.P. 1995. "On Estimation of the Wavelet Variance," *Biometrika*, **82**, pp. 619–631.
- [24] Perrier, V., Philipovitch, T., and Basdevant, C. 1995. "Wavelet Spectra Compared to Fourier Spectra," *Journal of Mathematical Physics*, **36**, pp. 1506–1519.
- [25] Verdant Power. 2010. Pilot License Application Roosevelt Island Tidal Energy Project. FERC No. 12611.

APPENDIX A: LINKAGES IN SPATIAL AND TEMPORAL SCALE OF PHYSICAL AND BIOLOGICAL PROCESSES AND MODELS.



RELATIONSHIP BETWEEN SPATIAL AND TEMPORAL SCALE. (TOP) FIGURE FROM STEELE ET AL. [16] DEMONSTRATING TEMPORAL-SPATIAL LINKAGES IN BOTH BIOLOGICAL AND PHYSICAL PROCESSES. (BOTTOM) FIGURE FROM WIENS [9] DEMONSTRATING STUDIES CONDUCTED AT FINE SPATIAL SCALES OVER LONG PERIODS OF TIME HAVE LOW PREDICTIVE POWER. STUDIES COVERING LARGER SPATIAL SCALES SHOULD BE CONDUCTED OVER COMPARABLE TEMPORAL SCALES.